ELSEVIER

Journal of Photochemistry and Photobiology A: Chemistry 133 (2000) 1–6

Journal of Photochemistry and Photobiology A:Chemistry

www.elsevier.nl/locate/jphotochem

Measurements of branching ratios of CaF($A^2\Pi_{1/2,1/3}$) from the reactions of Ca[4s4p(^3P_J)] with CH_3F following pulsed dye-laser excitation of atomic calcium

David Husain [a,*], Junfeng Geng [a], Fernando Castaño [b], Maria N. Sanchez Rayo [b]

[a] *Department of Chemistry, University of Cambridge, Lensfield Road, Cambridge CB2 1EW, UK*

[b] *Departamento de Quimica Fisica, Universidad del Pais Vasco, Apartado 644, 48080 Bilbao, Spain*

Received 25 November 1999; received in revised form 6 January 2000; accepted 6 January 2000

Abstract

Molecular electronic branching ratios to yield CaF($A^2\Pi_{1/2}$) and CaF($A^2\Pi_{3/2}$) have been measured in the time-domain following the F-atom abstraction reaction of electronically excited calcium atoms, Ca[4s4p(^3P_J)], 1.888 eV above the $4s^2$ ($^1S_0$) ground state, with $CH_3F^{\bullet}$ Ca[4s4p ($^3P_1$)] was generated by the pulsed dye-laser excitation of ground state calcium atoms at λ=657.3 nm {Ca[4s4p($^3P_1$)]←Ca[$4s^2$ ($^1S_0$)]} at elevated temperatures in the presence of CH_3F and excess helium buffer gas in a slow flow system, kinetically equivalent to a static system. Atomic fluorescence emission profiles at the resonance wavelength together with molecular chemiluminescence emissions at λ=606 nm, CaF($A^2\Pi_{1/2} \rightarrow X^2\Sigma^+$, $\Delta v = 0$) and λ=603 nm, CaF($A^2\Pi_{3/2} \rightarrow X^2\Sigma^+$, $\Delta v = 0$) were recorded. These demonstrated exponential decays characterised by decay coefficients which were equal under identical chemical conditions thus demonstrating the production of CaF($A^2\Pi_{1/2,3/2}$) by direct reaction of Ca(^3P_J) with CH_3F. The combination of the time-dependences of the atomic and molecular profiles as a function of the concentration of CH_3F together with integrated atomic and molecular intensities yielded branching ratios into the $A^2\Pi_{1/2}$ and $A^2\Pi_{3/2}$ states which were found to be as follows: $A_{1/2,}$ $(1.4\pm0.6)\times10^{-3}$; $A_{3/2}$, $(1.2\pm0.5)\times10^{-3}$. Whilst the higher lying CaF($B^2\Sigma^+$) is also energetically accessible on reaction, the B–X chemiluminescence was not observed and is attributed to a low branching ratio on reaction into that state. The results are compared with various related data for Ca(^3P_J) for total branching ratios into electronic states studied in the single collision condition and with branching ratios of SrF($A^2\Pi_{1/2}$, $A^2\Pi_{3/2}$, $B^2\Sigma^+$) following the reaction of Sr[5s5p(^3P_J)]+CH_3F investigated following pulsed dye-laser excitation where the yields of SrF($A_{1/2}$, $A_{3/2}$) were of similar low magnitudes.

Keywords: Laser excitation of Ca; Atomic fluorescence; CaF molecular chemiluminescence; Molecular electronic branching ratios

1. Introduction

The collisional behaviour of electronically excited calcium atoms in the Ca[4s4p(^3P_J)] state, 1.888 eV above the $4s^2$($^1S_0$) ground state [1], with alkyl halides has been investigated hitherto in the time-domain in order to study the mechanism of electronic energy distribution in the diatomic products following halogen atom abstraction [2–5]. The combination of time-resolved atomic fluorescence from Ca(4^3P_1) and time-resolved molecular chemiluminescence from CaX($A^2\Pi$, $B^2\Sigma^+ \rightarrow X^2\Sigma^+$) has thus been employed following the pulsed dye-laser generation of the atomic state. Such measurements are complementary to the study of analogous processes for electronically excited alkaline earth atoms using molecular beams under single-collision conditions [6–14] and is an area that has been reviewed in some detail from both the experimental and theoretical viewpoints [15–18]. Measurements of branching ratios into specific product quantum states for this type of chemical system for reactions of Ca(4^3P_J) in particular, whether from investigations in the time-domain or using single collision conditions, are limited. Dagdigian et al. [13] have studied the reactions of Ca(4^3P_J) with Cl_2, CH_3Cl, CH_3Br, CH_2Br_2, CH_2=$CHCH_2Br$ and $C_6H_5CH_2Br$ by the molecular beam technique. These authors report chemiluminescence cross sections [13] from which one can obtain total electronic branching ratios into all the accessible excited states, CaX($A^2\Pi_{1/2,3/2}$, $B^2\Sigma^+$). Gonzalez Ureña et al. [19] have studied the reactions Ca($^1D_2$, ^3P_J)+$CH_3I \rightarrow$ CaI(A,B)+CH_3 under beam-gas conditions and report an electronic branch-

* Corresopnding author. Fax: +44-1223-336362.

1010-6030/00/$ – see front matter
PII: S1010-6030(00)00211-2

ing ratio of r=CaI($A^2\Pi$)/CaI($B^2\Sigma^+$)=1.35 for Ca($^1D_2$) and Ca(^3P_J) in both cases.

Measurements of time-resolved atomic fluorescence and molecular chemiluminescence following the reaction of Ca(4^3P_J)+CH_3X (X=F, Cl, Br, I) [2–5] have been limited to comparisons of the time-dependences of the atomic and molecular profiles into the $A_{1/2}$, $A_{3/2}$ and B states. These indicate that CaX($A^2\Pi_{1/2,3/2}$, $B^2\Sigma^+$) arise from direct reaction rather than secondary processes involving electronic energy transfer and can thus be related to analogous studies on energy distribution in molecular beams. This is contrast to analogous measurements in the time-domain on the reactions Sr(5^3P_J) [20–23], 1.807 eV above the $5s^2(^1S_0)$ ground state, where branching ratios were also reported. In this paper we describe molecular electronic branching ratio measurements yielding CaF($A^2\Pi_{1/2,3/2}$) following the reactions of Ca(4^3P_J) with CH_3F. In further contrast to the earlier time-dependent measurements on Ca(4^3P_J)+CH_3F [2], improvements in data capture and subsequent computerised analysis has permitted optical resolution of the chemiluminescence components for the two spin–orbit states, CaF[($A^2\Pi_{1/2,3/2}$)→$X^2\Sigma^+$]. Chemiluminescence from CaF($B^2\Sigma^+\rightarrow X^2\Sigma^+$), which is energetically accessible, was not observed as also found in the earlier time-dependent measurements [2], clearly on account of the particularly low branching ratio into this state. The results are compared with related results for reactions of Ca(4^3P_J) in molecular beams and branching ratio measurements for Sr(5^3P_J) with halides in the time-domain [20–23], particularly the production of SrF($A^2\Pi_{1/2,3/2}$, $B^2\Sigma^+$) from the reactions of Sr(5^3P_J) with CH_3F [19].

2. Experimental details

The general experimental arrangement for monitoring atomic resonance fluorescence and molecular chemiluminescence in the time-domain following the reaction of Ca(4^3P_J) with CH_3F is a combination of that described hitherto for this atomic state [2–5] together with that used for the study of Sr(5^3P_J) and leading to molecular electronic branching ratios [20–23]. Ca[4s4p($^3P_1$)] was generated by the pulsed dye-laser excitation (10 Hz) of calcium vapour at elevated temperature (T=940 K) at λ=657.3 nm {Ca[4s4p($^3P_1$)]←Ca[$4s^2(^1S_0)$]} in the presence of methyl fluoride and excess helium buffer gas. Atomic emission at the resonance wavelength and molecular chemiluminescence from the states CaF[($A^2\Pi_{1/2,3/2}$, $B^2\Sigma^+\rightarrow X^2\Sigma^+$)] were then monitored using the standard combination of a small monochromator and a photomultiplier under identical chemical conditions. By contrast with earlier studies on Ca(^3P_J) using boxcar integration [2–5], atomic and molecular emission profiles were recorded by data capture of the complete profiles for each individual decay using a two-channel transient digitiser (Digital Storage Adapter, Thurlby DSA 524). The number of decay profile averaged was 256 as were the number of background profiles before subtraction and interfaced into a computer for data analysis. The materials (Ca, 99%; He, 99.999%; CH_3F Aldrich) were employed essentially as described in a previous investigation [2].

The optical and detection system was calibrated both with respect to electronic gain and wavelength sensitivity. The gain (G) for the PMT (E.M.I., 9797B) as a function of voltage was taken from the commercial calibration expressed in the form $\ln G = 8.7 \ln V - 54.4$ where G is in arbitrary units and V in volts [24]. The wavelength response of the photomultiplier-grating combination which employed a 'Minichrom' monochromator (MC1-02-10288, Fastie–Ebert mounting) was calibrated against a 'xenophot' lamp that had, in turn, been calibrated against a spectral radiometer (International Light Inc., USA IL 783). This yielded two peaks in the sensitivity response curve, one at ca. 460 nm and the other at ca. 540 nm [20–23], representing the expected combination of the grating response for the monochromator and the maximum response for the PMT. For the purpose of comparing time-dependent profiles, the sensitivity calibrations were not necessary. They were, however, required for the purpose of determining branching ratios into the specific electronic states where the atomic and molecular emissions needed to be placed on a common relative scale. In contrast to the previous time-resolved investigation on Ca(^3P_J)+CH_3F using the largest pair of slits (600 μm) for the monochromator [2], a smaller pair of slits (300 μm) were employed in these measurements in order to increase the wavelength resolution for the recorded chemiluminescence profiles and thus to isolate the two very close-lying spin–orbit components of CaF($A^2\Pi$). Whilst the data capture system using the transient digitiser described above was more efficient than boxcar integration, with recording of the complete emission profiles, the use of smaller slits, necessary for optical isolation of the chemiluminescence of the molecular spin–orbit components yielded significant noise in the molecular profiles, magnified when integrated. Nevertheless, it was possible to characterise the molecular electronic branching ratios on reaction of Ca(4^3P_J)+CH_3F.

3. Results and discussion

3.1. Time dependence of the atomic fluorescence, Ca[4s4p($^3P_1$)→$4s^2(^1S_0)$], and the molecular chemiluminescence, CaF($A^2\Pi_{1/2}$, $A^2\Pi_{3/2}\rightarrow X^2\Sigma^+$)

An example of the digitised output showing the time-resolved variation of the intensity of the atomic fluorescence emission {Ca[4s4p($^3P_1$)]→Ca[$4s^2(^1S_0)$]} at λ=657.3 nm following pulsed dye-laser excitation of calcium vapour at T=940 K in the presence of CH_3F and excess helium buffer gas is shown in Fig. 1a The first-order decay profile constructed from this exponential plot is given

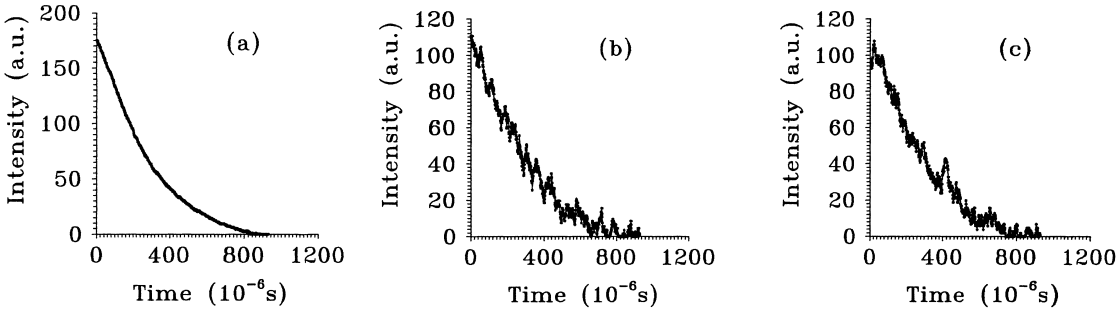

Fig. 1. Examples of the digitised output indicating the exponential decay profiles for the time-resolved atomic fluorescence emission and the molecular chemiluminescence following the pulsed dye-laser excitation of calcium vapour at the resonance wavelength {Ca[4s4p(^{3}P$_1$)]←Ca[4s2(^{1}S$_0$)], λ=657.3 nm} in the presence of CH_3F and excess helium buffer gas at elevated temperature. T=940 K. [CH_3F]=1.5×10^{16} molecules cm^{-3}, $p_{\text{TotalwithHe}}$=60 Torr. (a) Ca[4s4p(^{3}P$_1$)]→Ca[4s^2(^{1}S$_0$)], λ=657.3 nm; (b) CaF($A^2\Pi_{1/2}\rightarrow X^2\Sigma^+$, Δv=0 606 nm); (c) CaF($A^2\Pi_{3/2}\rightarrow X^2\Sigma^+$, Δv=0 603 nm).

in Fig. 2a though the first-order decay coefficient, k', is determined from computerised fitting of the raw data in Fig. 1a. Boltzmann equilibrium within the three spin–orbit levels of Ca(^{3}P$_{0,1,2}$) is rapidly established on the time scales of the present measurements by collisions with helium gas [25,26], in fact, this is further facilitated by the presence of a molecular reactant such as CH_3F. The first-order decay of Ca(4^3P$_J$) in the presence of CH_3F (Fig. 2a) can thus be expressed as

$$[\text{Ca}(^3\text{P}_J)]_t = [\text{Ca}(^3\text{P}_J)]_{t=0} \exp(-k't) \quad (1)$$

The first-order decay coefficient, k', may sensibly be given by the expression:

$$k' = \frac{A_{nm}}{(1 + 1/K_1 + K_2)} + \frac{\beta}{p_{\text{He}}} + \sum \text{k}_\text{Q}[\text{Ca}(^1\text{S}_0), \text{He}] + k_\text{R}\varepsilon[\text{CH}_3\text{F}] \quad (2)$$

where symbols have their usual meaning. A_{nm} (=1/τ_e) is the Einstein coefficient for emission from Ca(^{3}P$_1$), K_1 and K_2 represent equilibrium constants connecting the ^{3}P$_0$ and ^{3}P$_1$ states, and the ^{3}P$_1$ and ^{3}P$_2$ states, readily calculated by statistical thermodynamics at a given temperature, and the term in β describes diffusional loss out of the region optical observation. k_R is the absolute second-order rate constant for the total collisional removal of Ca(^{3}P$_J$) by CH_3F. The term involving $\sum k_Q$ describes collisional quenching of Ca(^{3}P$_J$) principally by ground state calcium atoms.

The true concentration of CH_3F molecules in the excitation region of the reactor is unknown due to the loss of this species by reaction with gaseous ground state Ca(^{1}S$_0$) atoms [27] before entry into the region of optical laser excitation. However, the determination of the mechanism of this reaction system and the branching ratios relies on comparisons between the first-order decay coefficients of the atomic and molecular emission profiles under identical conditions. The absolute concentration of CH_3F is not required. Characterisation of the branching ratios depends on a monotonic variation of k' and [CH_3F] which is established (see later). This is parameterised using ε, the fraction of the initial [CH_3F] entering the excitation zone which, within experimental error, is a constant in these measurements (see later). At constant total pressure, fixed temperature and fixed laser pulse output, Eq. (2) may be simplified as

$$k' = K + k_\text{R}\varepsilon[\text{CH}_3\text{F}] \quad (3)$$

where K is a constant. Fig. 3 shows the variation of k' with [CH_3F] (initial) but this cannot be used to determine an accurate value of the rate constant for the reaction of Ca(^{3}P$_J$) with CH_3F for the reasons given. For estimating

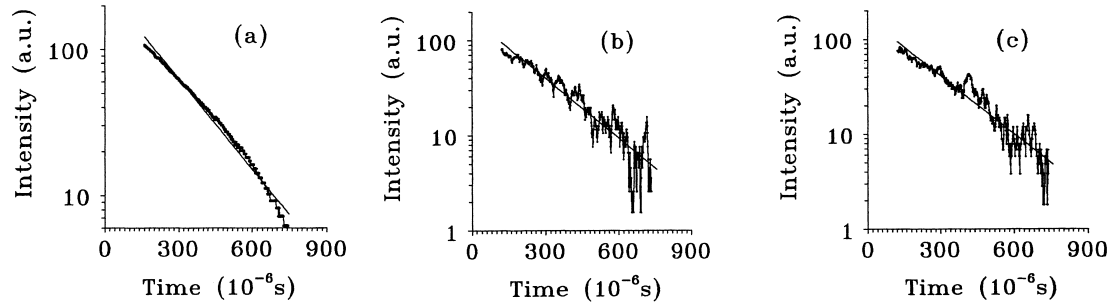

Fig. 2. Examples of the computerised fitting indicating the first-order decay profiles of the time-resolved atomic fluorescence emission and the molecular chemiluminescence following the pulsed dye-laser excitation of calcium vapour at the resonance wavelength {Ca[4s4p(^{3}P$_1$)]←Ca[4s^2(^{1}S$_0$)], λ=657.3 nm} in the presence of CH_3F and excess helium buffer gas at elevated temperature. T=940 K. [CH_3F]=1.5×10^{16} molecules cm^{-3}, $p_{\text{TotalwithHe}}$=60 Torr. (a) Ca[4s4p(^{3}P$_1$)]→Ca[4s2(^{1}S$_0$)], λ=657.3 nm;(b) CaF($A^2\Pi_{1/2}\rightarrow X^2\Sigma^+$, Δv=0.606 nm); (c) CaF($A^2\Pi_{3/2}\rightarrow X^2\Sigma^+$, Δv=0.603 nm).

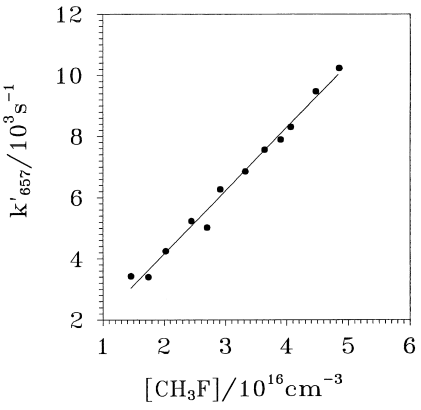

Fig. 3. Variation of the pseudo first-order rate coefficient, k'_{657}, for the decay of Ca(4^3P_J) in the presence of CH_3F at elevated temperature following pulsed dye-laser excitation of calcium vapour at the resonance wavelength {Ca[4s4p($^3P_1$)]←Ca[4s2($^1S_0$)], λ=657.3 nm} at elevated temperature. T=940 K. $p_{TotalwithHe}$=60 Torr.

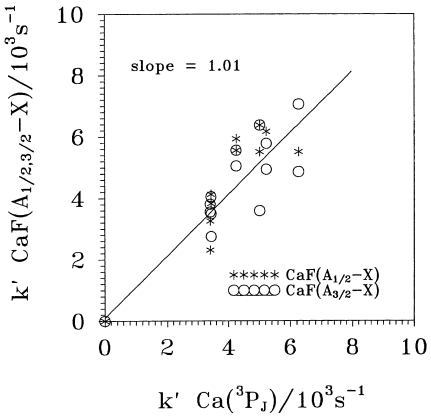

Fig. 4. Comparison of the first-order rate coefficients for the time-resolved molecular chemiluminescence from CaF($A^2\Pi_{1/2,3/2}\rightarrow X^2\Sigma^+$) and the time-resolved atomic fluorescence emission from Ca(4^3P_1) at λ=657.3 nm following the pulsed dye-laser excitation of calcium vapour at the resonance wavelength {Ca[4s4p($^3P_1$)]←Ca[4s2($^1S_0$)], λ=657.3 nm} in the presence of varying concentrations of CH_3F and excess helium buffer gas at elevated temperature. T=940 K. $p_{TotalwithHe}$=60 Torr.

branching ratios into the $A^2\Pi_{1/2}$ and $A^2\Pi_{3/2}$ states of CaF this monotonic variation of k' with [CH_3F] is the principal requirement.

Fig. 1b gives an example of the digitised output for the chemiluminescence emission from CaF($A^2\Pi_{1/2}\rightarrow X^2\Sigma^+$, Δv=0, λ=606 nm) under identical conditions to those given for the atomic emission from Ca[4s4p($^3P_1$)] and Fig. 2b, the associated computerised first-order decay profile. Analogous plots are given in Fig. 2c and 3c for the chemiluminescence arising from the close-lying $A^2\Pi_{3/2}$ state [28] at λ=603 nm (Δv=0). Chemiluminescence measurements are essentially restricted to Δv=0 sequences for the A–X system. Franck–Condon factors described hitherto in measurements restricted to time-resolved chemiluminescence measurements on the unresolved spin–orbit pair [2] $A^2\Pi$-$X^2\Sigma^+$ indicate that the intensity is mostly located in the (0,0) transition (f(0,0)=0.97882, f(0,1)=0.02116) [28–30]. More detailed measurements have recently been described by Field et al. on the CaF(A–X) system [31] where the interatomic distances indicate that intensity will be concentrated in the Δv=0 sequence (r_e/nm: $A^2\Pi$, 0.1937; $X^2\Sigma^+$, 0.1955). Fig. 4 shows the correlation between the first-order decay coefficients for the $A_{1/2,3/2}$–X emissions and those for the atomic emissions taken under identical conditions. The slope of the fitting is found to be 1.0, unity within experimental error, large on account of the necessity of using small slits to resolve the spin–orbit components of the weak emission from the molecular state. The 1σ error is considered to be ca. 10% for the slope as the plot is placed through the origin which is a physically realistic point. It may therefore be concluded that the atomic and molecular decay profiles are exponential in character and characterised by equal first-order decay coefficients following the direct reaction Ca(^3P_J)+CH_3F→CaF($A^2\Pi$, $X^2\Sigma^+$)+CH_3 (see later).

The $A^2\Pi_{1/2}$ (2.044 eV), $A^2\Pi_{3/2}$ (2.053 eV) and $B^2\Sigma^+$ (2.336 eV) states of CaF [32] are energetically accessible on collision of Ca(^3P_J) with CH_3F.

$$Ca\left(^3P_J\right) + CH_3F \rightarrow CaF\left(X^2\Sigma^+\right) + CH_3$$
$$\Delta H = -241.4\,kJ\,mol^{-1}$$

$$Ca\left(^3P_J\right) + CH_3F \rightarrow CaF\left(A^2\Pi_{1/2}\right) + CH_3$$
$$\Delta H = -44.2\,kJ\,mol^{-1}$$

$$Ca\left(^3P_J\right) + CH_3F \rightarrow CaF\left(A^2\Pi_{3/2}\right) + CH_3$$
$$\Delta H = -43.4\,kJ\,mol^{-1}$$

$$Ca\left(^3P_J\right) + CH_3F \rightarrow CaF\left(B^2\Sigma^+\right) + CH_3$$
$$\Delta H = -16.0\,kJ\,mol^{-1}$$

(D^0_0[CaF($X^2\Sigma^+$)]=5.506±0.09 eV [33]; D^0_{298}[CH_3F]= 472 kJ mol^{-1} [34]; $\omega_e(A_{1/2})$=586.8 cm^{-1}, $\omega_e(A_{3/2})$=593.4 cm^{-1}, ω_e(B)=566.1 cm^{-1}, [32]). These molecular states cannot be generated by electronic energy transfer between Ca(^3P_J) (1.888 eV, [1]) and ground state CaF($X^2\Sigma^+$, v″=0) resulting from the overall reaction. Some level of vibrational excitation in CaF($A^2\Pi_{1/2}$, v′≤6; $A^2\Pi_{3/2}$, v′≤5) and also CaF($B^2\Sigma^+$, v′≤2) is energetically possible on initial reaction. Chemiluminescence from the $B^2\Sigma^+$–$X^2\Sigma^+$ system of CaF((0,0), 531 nm), however, was not observed from which it may be concluded that the branching ratio into the B state is very low, consistent with the observed low branching ratios into the lower lying $A_{1/2}$ and $A_{3/2}$ states.

3.2. Molecular electronic branching ratios

Molecular electronic branching ratios into CaF($A_{1/2}$, $A_{3/2}$) from the reaction Ca(^3P_J)+CH_3F may be determined

using measurements of the integrated atomic and molecular intensities derived from the recorded decay profiles. The appropriate rate equations are presented here without immediate correction for the response of the optical system at different wavelengths and the electronic gain of the photomultiplier at different operating voltages but these corrections are included when using the final values of the integrated intensities. The first-order decay coefficient for [Ca(^3P_J)], k', following Eq. (1) has been given in Eqs. (2) and (3). Noting that atomic emission only arises essentially from one spin–orbit level, $^3P_1$, in the Ca(^3P_J) manifold [35], the atomic emission intensity is given by the form [2–5]:

$$I_{em}(^3P) = \left(\frac{A_{nm}}{F}\right)[Ca(^3P_J)]_{t=0}\exp(-k't)\mathfrak{A} \quad (4)$$

where $A_{nm}=1/\tau_e$ for Ca($^3P_1$-$^1S_0$) and $F=(1+1/K_1+K_2)$ [1–4]. The integrated atomic intensity is then given by

$$I(^3P_J) = \frac{A_{nm}[Ca(^3P_J)]_{t=0}}{k'F} \quad (5)$$

The short mean radiative lifetimes of CaF($A^2\Pi_{1/2}$, $A^2\Pi_{3/2}$), characterised by Dagdigian et al. [36] (τ_e'/ns: $A^2\Pi_{1/2}$ 21.9±4.0, $A^2\Pi_{3/2}$ 18.4±4.1), clearly permit the concentrations of the $A_{1/2}$ and $A_{3/2}$ states to be placed in steady state following their direct production within the time-scales employed in the present investigation. In the case of CaF($A_{1/2}$) resulting from the reaction of Ca(^3P_J)+CH_3F, the steady state expression is given by

$$-\frac{d[CaF(A_{1/2})]}{dt} = k_1[Ca(^3P_J)]\varepsilon[CH_3F] - A'_{nm}[CaF(A_{1/2})] = 0 \quad (6)$$

where $A'_{nm}=1/\tau'_e$ for CaF($A^2\Pi_{1/2}$). The molecular emission intensity from CaF($A_{1/2}$–X) is thus readily given by

$$I_{em}(A_{1/2}-X) = k_1\varepsilon[CH_3F][Ca(^3P_J)]_{t=0}\exp(-k't) \quad (7)$$

where k_1 is the rate constant for the production of CaF($A^2\Pi_{1/2}$). Thus, the equality of the exponential time-dependences of the atomic emission (Eq. (4)) and the molecular chemiluminescence (Eq. (7)) are in accord with the production of CaF($A^2\Pi_{1/2}$) by direct reaction between Ca(4^3P_J) and CH_3F. Following Eq. (7), the integrated molecular intensity is given by

$$I(A_{1/2}-X) = \frac{k_1\varepsilon[CH_3F][Ca(^3P_J)]_{t=0}}{k'} \quad (8)$$

Thus, from Eqs (5) and (8), the ratio of the integrated molecular intensity for CaF($A_{1/2}$–X), for example, to that of the ($^3P_1$–$^1S_0$) atomic fluorescence emission is then given by

$$\frac{I(A_{1/2}-X)}{I(^3P_J)} = k_1\varepsilon\left(\frac{F}{A_{nm}}\right)[CH_3F] \quad (9)$$

Hence, it may further be seen that the ratio of the slopes of the plots of (1): $I(A_{1/2}-X)/I(^3P_J)$ versus [CH_3F] (Fig. 5a)

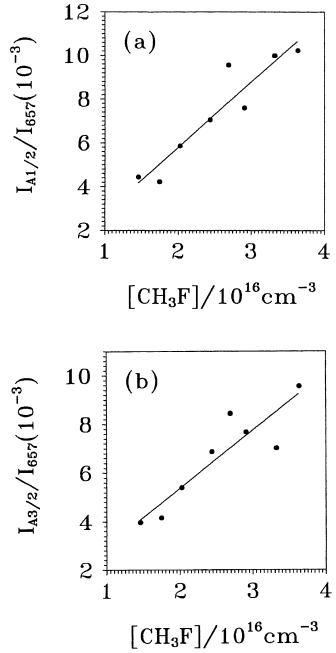

Fig. 5. Variation of the integrated intensity ratios of the molecular chemiluminescence emissions to the atomic fluorescence emission Ca($4^3P_1\rightarrow4^1S_0$) (λ=657.3 nm) for (a) CaF($A^2\Pi_{1/2}\rightarrow X^2\Sigma^+$, Δv=0, λ=606 nm) and (b) CaF($A^2\Pi_{3/2}\rightarrow X^2\Sigma^+$, Δv=0, λ=603 nm) as a function of the concentration of CH_3F following the pulsed dye-laser excitation of calcium vapour at the resonance wavelength (λ=657.3 nm) in the presence of excess helium buffer gas at elevated temperature. (T=940 K, $p_{TotalwithHe}$=60 Torr).

and (2) k' versus [CH_3F] (Fig. 3), yields the branching ratio for the formation of CaF($A^2\Pi_{1/2}$), namely,

$$r_{A_{1/2}} = \left(\frac{A_{nm}}{F}\right)\frac{\text{slope}(1)}{\text{slope}(2)} \quad (10)$$

where $r_{A_{1/2}}=k_1/k_R$, the rate of production of CaF($A^2\Pi_{1/2}$) from the reaction of Ca(^3P_J) by CH_3F relative to the total removal rate of Ca(^3P_J) by this molecule.

A_{nm} has been characterised separately in this work from measurements of atomic decay profiles similar to that in Fig. 1a at different temperatures yielding $\tau_e=1/A_{nm}=0.36$ ms, a value in very close accord with a wide range of measurements obtained in the time-domain [15]. $F=1+1/K_1+K_2=2.778$ at T=940 K, calculated by statistical thermodynamics. The branching ratio into CaF($A^2\Pi_{3/2}$) can be calculated on the same basis as for the $^2\Pi_{1/2}$ state and thus the relevant plot for component (1) is given in Fig. 5b. The branching ratios into the excited states obtained in this investigation are found to be as follows: $A_{1/2}$, $(1.4\pm0.6)\times10^{-3}$; $A_{3/2}$, $(1.2\pm0.5)\times10^{-3}$. The errors quoted here arise mainly arise from the errors of the slopes of the plots in Fig. 5a and b High accuracy is not claimed for these slopes in view of the limitations, necessarily encountered in the measurements of the integrated molecular intensities. Nevertheless, these branching ratios do constitute, to the best of our knowledge, the first measurements of such prod-

uct branching ratios for reactions of $Ca(^3P_J)$ with a halide obtained in the time-domain, and particularly for measurements of specific molecular spin–orbit states of $CaF(A^2\Pi)$. In fundamental terms, at the minimum level, branching ratios could be rationalised in terms of the symmetry of the appropriate potential surfaces using correlation diagrams, however, in this instance, C_s symmetry would not constitute the least symmetrical complex for a five-atom intermediate. The total yield, $\sum(CaF(A_{1/2}, A_{3/2})) = 2.6 \times 10^{-3}$, can only be compared with analogous data reported by Husain et al. [20] for the reaction of $Sr(5^3P_J)+CH_3F$ and found to be ca. 7.9×10^{-3} for $SrF(A_{1/2}+A_{3/2})$. A branching ratio for $SrF(B^2\Sigma^+)$ of 1.1×10^{-4} was also reported in that work [20]. In experimental terms, whilst comparable branching ratios are observed for the analogous states of SrF [20], measured atomic and molecular emission intensities will be higher in that case on account of the higher initial densities of $Sr(5^3P_1)$ generated from laser excitation resulting from the shorter mean radiative lifetime of $Sr(5^3P_1)$ [20]. Finally, assuming that removal of $Ca(^3P_J)+CH_3F$ proceeds entirely by F-atom abstraction into $CaF(A_{1/2}, A_{3/2}, X)$ given no detection of B–X chemiluminescence and higher states of CaF not being energetically accessible, one may, in turn, estimate an upper limit for the branching ratio into the product ground state $CaF(X^2\Sigma^+)$ of ca. 99.7% in view of the possible role of physical quenching of $Ca(4^3P_J)$ by CH_3F into $Ca(4^1S_0)$.

Acknowledgements

We thank the Sino–British Friendship Scholarship Scheme for a scholarship held by J.G. during the tenure of which this work was carried out. We are also indebted to Dr. Jie Lei and Dr. G.A. Jones of D.E.R.A. (Fort Halstead) for encouragement and helpful discussions.

References

[1] C.E. Moore (Ed.), Atomic Energy Levels, Nat. Bur. Stand. Ref. Data Ser., Vol. 35, Parts I–III, U.S. Government Printing Office, Washington, DC, 1971.
[2] F. Beitia, F. Castaño, M.N. Sanchez Rayo, S.A. Carl, D. Husain, J. Photochem. Photobiol. Chem. A 62 (1991) 1.
[3] F. Beitia, F. Castaño, M.N. Sanchez Rayo, S.A. Carl, D. Husain, J. Chem. Soc., Faraday Trans. 87 (1991) 2413.
[4] F. Beitia, F. Castaño, M.N. Sanchez Rayo, S.A. Carl, D. Husain, L. Santos, Z. Phys. Chem. Neue Folge 171 (1991) 137.
[5] F. Beitia, F. Castaño, M.N. Sanchez Rayo, S.A. Carl, D. Husain, Ber. Bunsenges. Phys. Chem. 95 (1991) 1615.
[6] P.J. Dagdigian, M.L. Campbell, Chem. Rev. 87 (1987) 1.
[7] R.W. Solarz, S.A. Johnson, J. Chem. Phys. 70 (1979) 3592.
[8] E. Verdasco, V.S. Rabanoz, F.J. Aoiz, A. Gonzalez Ureña, J. Phys. Chem. 91 (1987) 2073.
[9] T. Kiang, R.C. Estler, R.N. Zare, J. Chem. Phys. 70 (1979) 5925.
[10] T. Kiang, R.N. Zare, J. Am. Chem. Soc. 102 (1980) 4024.
[11] H. Yuh, P.J. Dagdigian, J. Chem. Phys. 81 (1984) 2375.
[12] P.J. Dagdigian, in: A. Fontijn (Ed.), Gas Phase Chemiluminescence and Chemi-ionisation, North Holland, Amsterdam, 1985, Chapter 11, p. 203.
[13] N. Furio, M.L. Campbell, P.J. Dagdigian, J. Chem. Phys. 84 (1986) 4332.
[14] M.L. Campbell, N. Furio, P.J. Dagdigian, Laser Chem. 6 (1986) 391.
[15] D. Husain, G. Roberts, in: J.E. Baggott, M.N. Ashfold (Eds.), Bimolecular Collisions, Advances in Gas-Phase. Photochemistry and Kinetics, Royal Society of Chemistry, London, 1989, p. 263.
[16] W.H. Breckenridge, H. Umemoto, Adv. Chem. Phys. 50 (1982) 325.
[17] W.H. Breckenridge, in: A. Fontijn, M.A.A. Clyne (Eds.), Reactions of Small Transient Species: Kinetics and Energetics, Academic Press, London, 1983, p. 157.
[18] D. Husain, J. Chem. Soc., Faraday Trans. 2 (1989) 85.
[19] J.M. Orea, A. Laplaza, C.A. Rinaldi, G. Tardajos, A. Gonzalez Ureña, Chem. Phys. 220 (1997) 337.
[20] S. Antrobus, S.A. Carl, D. Husain, J. Lei, F. Castaño, M.N. Sanchez Rayo, Ber. Bunsenges. Phys. Chem. 99 (1975) 127.
[21] S. Antrobus, D. Husain, J. Lei, F. Castaño, M.N. Sanchez Rayo, Int. J. Chem. Kinet. 27 (1995) 741.
[22] S. Antrobus, D. Husain, J. Lei, F. Castaño, M.N. Sanchez Rayo, J. Chem. Res. 84 (1995) 601.
[23] S. Antrobus, D. Husain, J. Lei, F. Castaño, M.N. Sanchez Rayo, Z. Phys. Chem. 190 (1995) 267.
[24] E.M.I. Catalogue, E.M.I. Industrial Publications, 1979.
[25] F. Beitia, F. Castaño, M.N. Sanchez Rayo, D. Husain, Chem. Phys. 166 (1992) 275.
[26] T.J. McIlrath, J.L. Carlsten, J. Phys. B 6 (1973) 697.
[27] R.S. Clay, D. Husain, Combustion and Flame 86 (1991) 371.
[28] R.P. Tuckett, private communication with D. Husain, 1992.
[29] R.W. Field, D.O. Harris, T. Tanaka, J. Mol. Spectrosc. 57 (1975) 107.
[30] J. Nakagawa, P.J. Domaille, T.C. Steimle, D.O. Harries, J. Mol. Spectrosc. 70 (1978) 374.
[31] L.A. Kaledin, J.C. Bloch, M.C. McCarthy, R.W. Field, J. Mol. Spectrosc. 197 (1999) 287.
[32] K.P. Huber, G. Herzberg, Molecular Spectra and Molecular Structure IV: Constants of Diatomic Molecules, Van Nostrand Reinhold, New York, 1979.
[33] Z. Karney, R.N. Zare, J. Chem. Phys. 68 (1970) 3360.
[34] David R. Lide (Ed.), 78th CRC Handbook of Chemistry and Physics, 1997, pp. 9–66.
[35] W.L. Wiese, M.W. Smith, B.M. Miles, Atomic Transition Probabilities, NSRDS-NBS-22, U.S. Government Printing Office, Washington, DC, 1969, Vol. 2.
[36] P.J. Dagdigian, H. Cruse, R.N. Zare, J. Chem. Phys. 60 (1974) 2330.